

SYNTHESIS AND CHARACTERIZATION OF SILVER-DOPED HYDROXYAPATITE

Regina PETKES^a, Noémi-Izabella FARKAS^a,
Laura MARINCAȘ^a, Judith-Hajnal BARTHA-VARI^a,
Réka BARABÁS^{a,*}

ABSTRACT. Different preparation methods of Ag-doped hydroxyapatite were compared and an efficient solid-state reaction-based method was developed for the synthesis of silver doped-hydroxyapatite using AgNO₃ as silver source. The obtained nanomaterial was characterized by SEM, EDS and XRD measurements. By this method 10% silver was detected in the structure of the hydroxyapatite.

Keywords: hydroxyapatite, silver, silver-doped hydroxyapatite, wet precipitation method, solid state method

INTRODUCTION

The globally increasing antibiotic-resistant infections drove the interest toward developing alternative bactericidal materials [1].

Silver is a highly effective natural antibacterial agent that can interact with a wide range of organisms such as viruses [2], bacteria [3] and fungi [4]. It has excellent biocompatibility, satisfactory stability and low toxicity to mammalian cells [5]. Due to these properties, silver nanoparticles appear in surgical instruments, medical catheters, antimicrobial dressings [6], but it can also be observed in many consumer articles such as cosmetics [7], detergents

^a Babeş-Bolyai University, Faculty of Chemistry and Chemical Engineering, Department of Chemistry and Chemical Engineering, Hungarian Line of Study 11 Arany Janos str., RO-400028, Cluj-Napoca, Romania

* Corresponding author: reka.barabas@ubbcluj.ro



[8], air and water filters [9], and various textiles. In the past years during the pandemic silver's antiviral property was intensely studied and found to be effective against SARS-CoV-2 [10], [11], [12].

Hydroxyapatite (HAP) is a calcium phosphate similar to human bone and teeth [13]. It has outstanding properties such as bioactivity, biocompatibility, osteoconductivity and affinity to biopolymers [14]. Hydroxyapatite is also nontoxic and has a non-inflammatory [15] non-allergenic, non-mutagenic nature [16]. Due to these unique properties, hydroxyapatite has got a variety of applications as biomedical material. It has been successfully applied in orthopedics, dentistry, ophthalmology, traumatology and maxillofacial surgery [17], but it is also used in medical devices [18] or in drug delivery systems [19]. The synthesis of HAP can be achieved by dry, wet and high temperature methods. The size, morphology and crystalline phase of the calcium phosphate will be different in case of the used synthesis method, which will affect the hydroxyapatite's properties [20]. It is important for hydroxyapatite-based nanomaterials used as implants to possess antibacterial properties; thus, the synthesis of silver doped nanomaterials is gaining more and more interest. The treatment duration can be reduced by the antibacterial effect, the efficacy of the implant can be thus improved. Silver can be incorporated in biomaterials including hydroxyapatite in its many oxidation states [21].

Among the most used processes the simple wet precipitation method is which, facilitates the incorporation of silver into the apatite structure. Although this method has advantages on industrial scale [22] the presence of potential impurities due to various ions manifested in aqueous solution can be a drawback.

Several wet methods were implied for doping hydroxyapatite with silver. Ciobanu et al. [23] used the coprecipitation method for synthesizing silver-doped hydroxyapatite. They studied its antimicrobial and antibacterial activity against fungi and bacteria. The same approach was used by Lim et al. [24] for the synthesis of silver decorated HAP. A low temperature ion-exchange technique was also used for the preparation of nano silver loaded hydroxyapatite [25]. Plasma spraying method was also used for doping hydroxyapatite with silver oxide [26]. Vukomanovic et al. [27] developed a sonochemical method for the growth of silver nanoparticles in combination with hydroxyapatite to form composites. Sol-gel approaches were used for doping hydroxyapatite with silver, Chen et al. evaluated the antibacterial property of Ag containing hydroxyapatite film on titanium surfaces obtained by this method [28].

Ag-doped hydroxyapatite was also prepared using microwave assisted synthesis [29], or ion beam-assisted deposition.

Based on our previous successful incorporation of doxycycline in HAP structure [30] in order to further enhance the antibacterial property of hydroxyapatite, the aim of the present study is the incorporation of silver in the structure of HAP using different methods and to compare the effectiveness of these methods.

RESULTS AND DISCUSSION

The aim of the study was a critical comparison of different methods for the synthesis of silver doped hydroxyapatite and the characterization of the obtained product.

In recent years, a variety of methods have been used for the synthesis of silver doped hydroxyapatite, such as hydrothermal, sol-gel, mechanochemical, ultrasonic and combustion processing. In all our attempts hydroxyapatite was prepared by *wet precipitation* method, a process efficiently controlled. Hydroxyapatite was prepared using $\text{Ca}(\text{NO}_3)_2$ and $(\text{NH}_4)_2\text{HPO}_4$. The calcium nitrate to diammonium phosphate ratio (Ca/P) was 1.67. During the preparation process the pH of the solution was maintained at 11 and for doping with Ag, different methods were used. Table 1 contains the obtained products and their naming.

Table 1. Methods used for the synthesis of silver-doped hydroxyapatite and the naming of the obtained products

NR.	METHOD	SILVER SOURCE	LABELING	
			Calcined	Non-calcined
1	Wet precipitation	Colloidal silver	<i>C-Ag-HAP-cal</i>	<i>C-Ag-HAP</i>
2	Wet precipitation	AgNO_3	<i>Ag-HAP-cal</i>	<i>Ag-HAP</i>
3	Wet precipitation	Silver complex	<i>Co-Ag-HAP-cal600</i> <i>Co-Ag-HAP-cal800</i>	<i>Co-Ag-HAP-noncal</i>
4	Solid state	AgNO_3	-	<i>Sp-Ag-HAP</i>

1. In our *first attempt* colloidal silver was used as silver source, which was obtained from AgNO_3 solution and NaBH_4 . The silver colloid was added to the hydroxyapatite solution and the reaction mixture was stirred continuously for 24 hours at room temperature. The silver doped HAP nanoparticles were dried at 200°C and half of the sample was calcined at 1000°C . The obtained nanoparticles were characterized by different physical-chemical methods. The morphology, particle size and chemical elemental composition of silver-doped HAP were observed by scanning electron microscopy coupled with

energy-dispersive X-ray diffraction (SEM/EDS). XRD measurements were also used for the analysis of the materials. The XRD spectra of the obtained nanomaterial is shown in **Figure 1**. For the non-calcined material (*C-Ag-HAP*) as well for the sintered (*C-Ag-HAP-cal*) the spectra shows the signal for hydroxyapatite and for the $\text{Ca}(\text{NO}_3)_2$, but the signal for the silver cannot be observed.

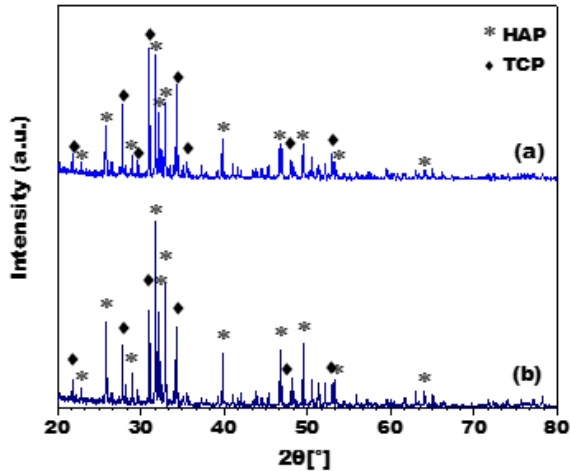


Figure 1. XRD diffractograms of (a) *C-Ag-HAP* and (b) *C-Ag-HAP-cal*

EDS measurements were also performed for both obtained samples (**Figure 2** and **Figure 3**): Large amounts of carbon, phosphorus and oxygen can be seen, but there the silver is not present in the samples.

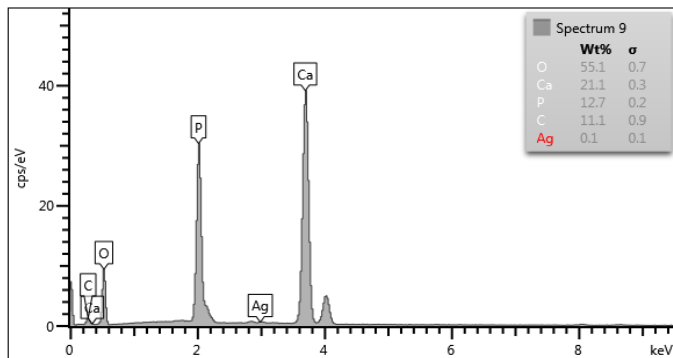


Figure 2. EDS measurements for the *C-Ag-HAP*

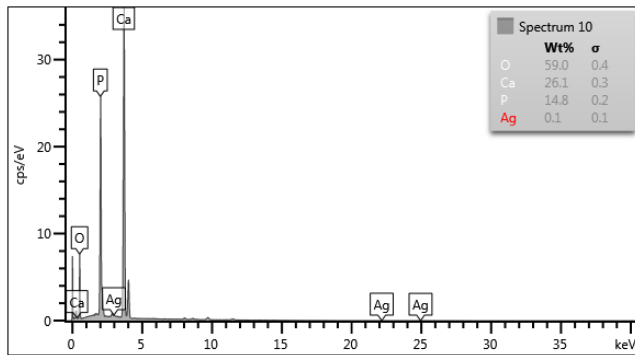


Figure 3. EDS measurements for the *C-Ag-HAP-cal*

2. In our *next attempt* for obtaining silver doped hydroxyapatite AgNO_3 was used as silver source. The solution of AgNO_3 was added to the solution of calcium nitrate tetrahydrate. To the resulting solution, the diammonium hydrogen phosphate solution was added using a peristaltic pump. The pH of the solution was adjusted to 11 and stirred continuously for 24 hours at room temperature. After the reaction time, the mixture was filtered under vacuum, washed with deionized water, dried at 200°C , and half of the sample was calcined at 1000°C (Ag-HAP and Ag-HAP-sint). These materials were also tested with XRD, but the results only show the signals for the hydroxyapatite both for the non-calcined and calcined materials (**Figure 4**).

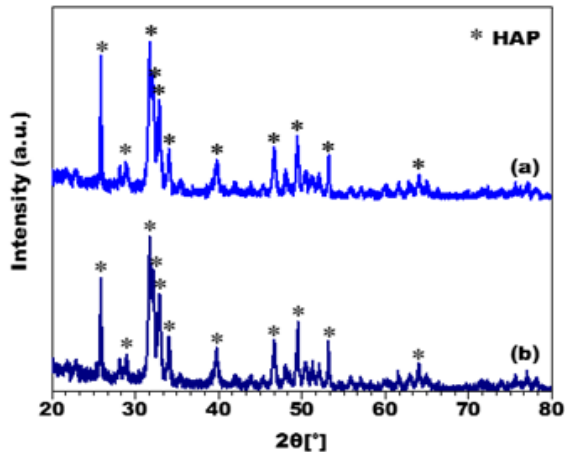


Figure 4. XRD diffractograms of (a) Ag-HAP and (b) Ag-HAP-cal

EDS analysis was also performed, but the silver could not be detected (Figure 5 and 6).

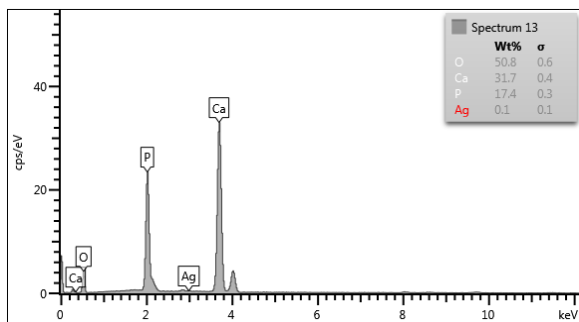


Figure 5. EDS spectra of Ag-HAP

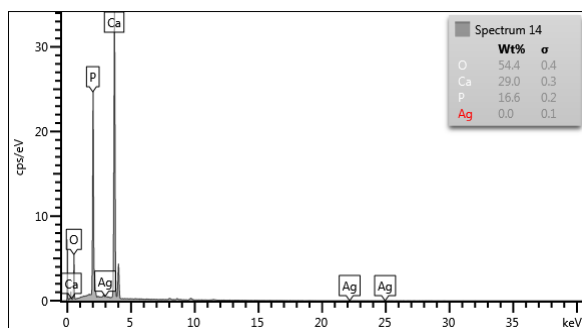
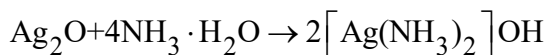
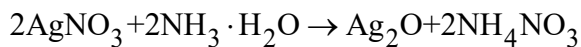


Figure 6. EDS spectra of Ag-HAP-cal

3. Further a diamine-silver hydroxide complex was used as silver source in order to incorporate the silver in the structure of the hydroxyapatite. For the preparation of the complex AgNO_3 solution was prepared and then ammonia solution was added until the silver oxide precipitated. The solution was centrifuged, the liquid phase removed, and the silver oxide was redissolved in 25 % ammonia solution (Scheme 1).



Scheme 1. Preparation of the silver complex

The solution of the formed complex was mixed with the solution of the hydroxyapatite. The pH of the reaction mixture was adjusted to 11 with ammonia solution, stirred continuously for 24 hours at room temperature, filtered, washed, dried and the resulting sample was then divided into three parts. The first sample was not calcined (*Co-Ag-HAP-noncal*), while the second and third samples were calcined at 600°C for 1 hour (*Co-Ag-HAP-sint600*). Afterwards, the third sample was calcined at 800°C for another 1 hour (*Co-Ag-HAP-sint800*). XRD spectra show no evidence of silver in the samples (**Figure 7**).

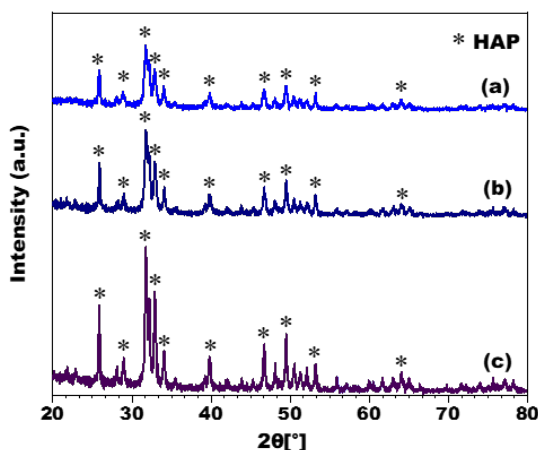


Figure 7. XRD diffractograms of (a) *Co-Ag-HAP-noncal*, (b) *Co-Ag-HAP-cal600*, and (c) *Co-Ag-HAP-cal800*

EDS measurements are in accordance with the XRD spectra, the amount of silver cannot be detected on the synthesized nanomaterials (**Figure 8, 9, 10**).

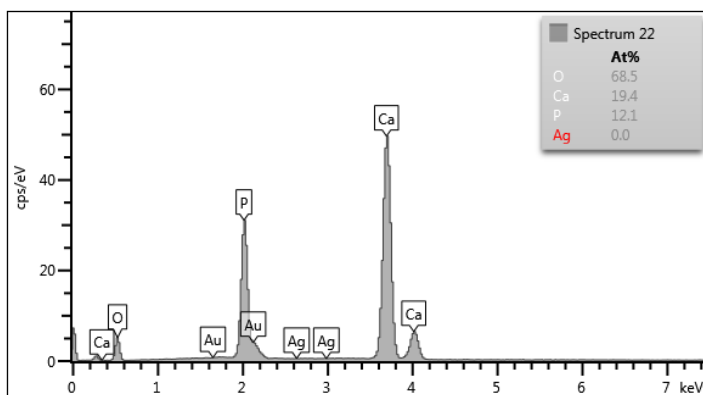


Figure 8. EDS spectra of *Co-Ag-HAP-noncal*

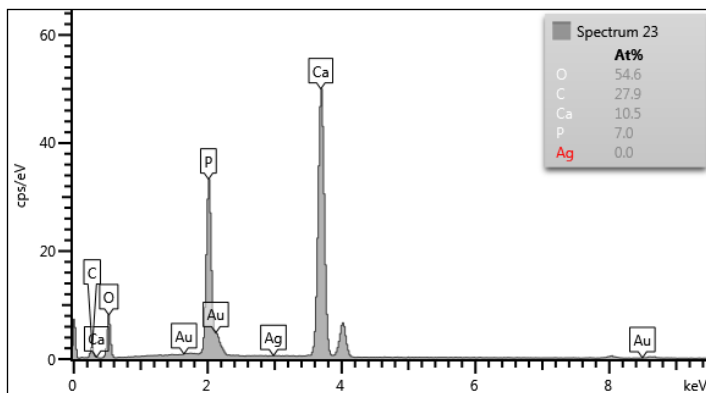


Figure 9. EDS spectra of *Co-Ag-HAP-cal600*

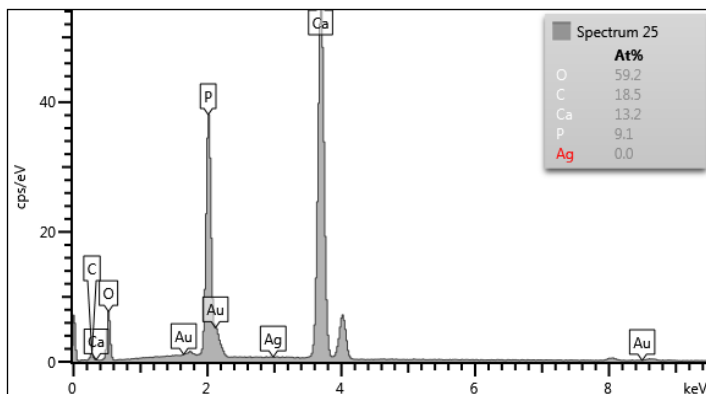


Figure 10. EDS spectra of *Co-Ag-HAP-cal800*

Although there are several examples in the literature which report the successful incorporation of silver into the hydroxyapatite's structure with the above described methods, we could not reproduce their results. According to Rajendran *et al.* silver cannot be incorporated into the hydroxyapatite's structure at pH 11 [31]. The article reports that systematic studies have been carried out to understand the effect of pH on silver precipitation in Ag-HAP nanomaterials. They concluded that silver can only precipitate on HAP if the pH of the mixing solution is 9 or below, but stable and pure HAP can only be synthesized at pH above 9.

4. Therefore, the *solid-state method* was tested for the preparation of silver doped hydroxyapatite.

Pure apatite was synthesized as earlier described. AgNO_3 was used as silver source which was added to the hydroxyapatite powder. The resulting mixture was calcined at 500°C for 1 hour and then 800°C for 1 hour (Sp-Ag-HAP). After calcination, the previously white sample turned brown. Using this method, on the XRD spectra also the silvers' signal is visible (**Figure 11**). The EDS analysis revealed 10% silver in the hydroxyapatite structure (**Figure 12**).

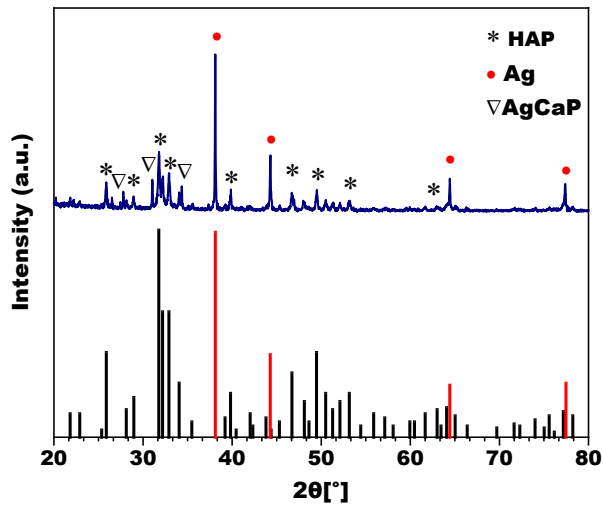


Figure 11. XRD diffractograms of Sp-Ag-HAP

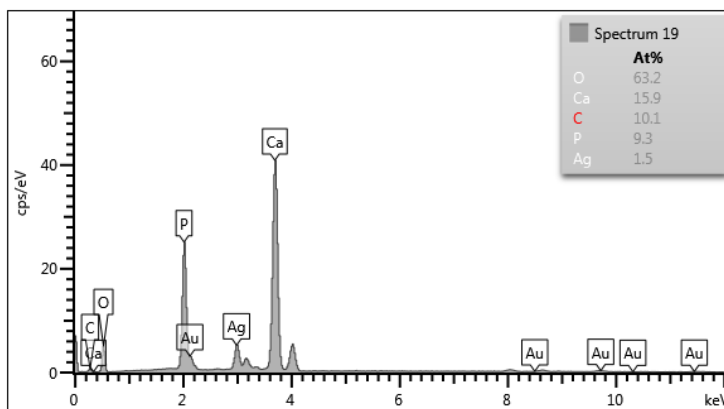


Figure 12. EDS spectra of Sp-Ag-HAP

The surface and the morphology of the obtained nanoparticles were also investigated with scanning electron microscopy (**Figure 13**). From the obtained images the Ag-hydroxyapatite granules and their rounded shape can be observed which were obtained by the sintering process.

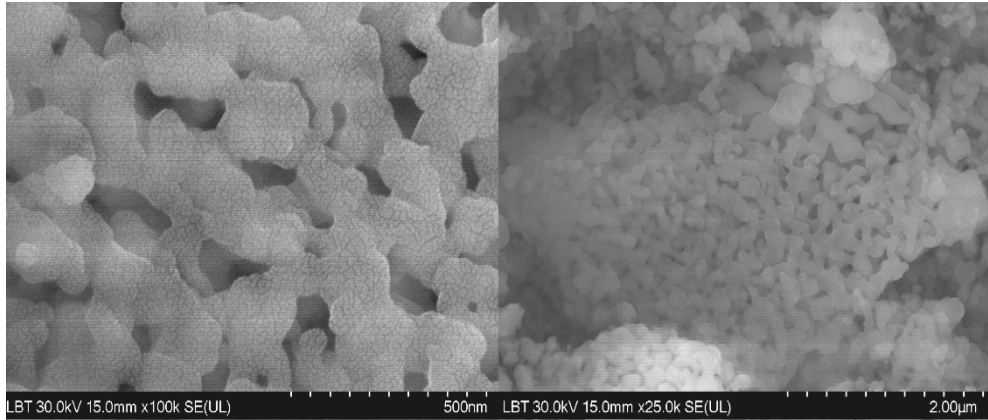


Figure 13. SEM images of the Sp-Ag-HAP nanoparticles

The EDS layered images are in accordance with the previously described observations, on the spectra of C-Ag-HAP (which was chosen as representative for the unsuccessful reactions), no silver can be observed, while the spectra of Sp-Ag-HAP reveal also the presence of silver (**Figure 14**).

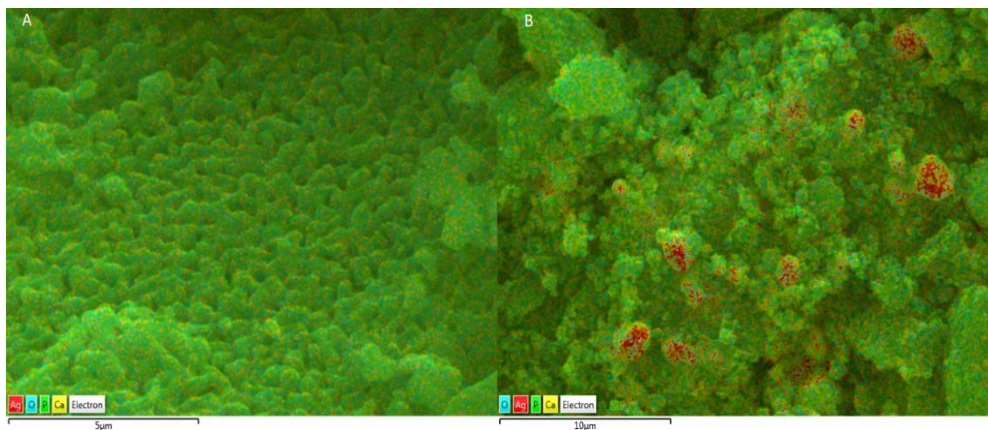


Figure 14. EDS images for (A) C-Ag-HAP and (B) Sp-Ag-HAP

CONCLUSIONS

In the present study our aim was the comparison of the methods used for the preparation of Ag-doped HAP. For this purpose, several methods (some of them can be also found in the literature) were employed using silver from different sources (colloidal silver, silver nitrate or silver complex). The obtained nanoparticles were characterized by SEM, EDS and XRD measurements. The solid-state method using AgNO_3 as silver source enabled the highest incorporated silver amount (10%). The obtained nanomaterial (Sp-Ag-HAP) could have potential application as a novel antimicrobial material.

EXPERIMENTAL SECTION

Materials

Chemicals

Calcium nitrate tetrahydrate ($\text{Ca}(\text{NO}_3)_2 \cdot 4\text{H}_2\text{O}$, (purity $\geq 99\%$), diammonium hydrogen phosphate ($(\text{NH}_4)_2\text{HPO}_4$, (purity $\geq 98.0\%$), ammonia solution (25%) were purchased from Carl Roth GmbH (Germany). Silver nitrate (AgNO_3 , purity $\geq 99\%$) and sodium borohydrate (NaBH_4 , purity $\geq 98\%$) are products of Sigma-Aldrich. All other reagents were of analytical grade (Merck, Germany) and used without further purification.

Equipments

The morphology, particle size and chemical elemental composition of silver-doped HAP were observed by scanning electron microscopy coupled with energy-dispersive X-ray diffraction (SEM/EDS). An Apreo SEM (Thermo Fisher, USA) equipped with Octane Elect EDS (AMETEK, USA) was used at 20.0 kV. The crystal structure was identified by X-ray diffraction (Bruker D8 Advance, Germany) with $\text{CuK}\alpha$ radiation ($\lambda=1.54060 \text{ \AA}$) operated at 40 kV and 40 mA.

The XRD analysis was performed on a Shimadzu XRD 6000 (Japan) using $\text{CuK}\alpha$ radiation at 40Kv, 30mA, at $\lambda=1.542 \text{ \AA}$. X-Ray images were prepared for each material. The red lines indicate the characteristic signs of the HAP crystals 25,8 32,05 39,84 46,78 49,53 53,13 63,97. The spectrum was identified by the ICPDS 09-0432 code in database.

Methods

Wet precipitation methods

1. Synthesis of colloidal silver-doped hydroxyapatite (C-Ag-HAP, C-Ag-HAP-sint)

For the synthesis of colloidal silver-doped hydroxyapatite the first step consisted of preparation of the silver source. 2 mL of an 1mM AgNO_3 solution cooled on ice was added to 30mL solution of NaBH_4 (2mM).

Hydroxyapatite was prepared according to our previously reported method [32],[33]. For preparation of HAP nanoparticles a 0.09M $(\text{NH}_4)_2\text{HPO}_4$ (250mL, pH 11) was added to a 0.15M $\text{Ca}(\text{NO}_3)_2$ (250mL, pH 11) solution using a peristaltic pump with a flow rate of 25mL/min. The colloidal silver solution was added to the hydroxyapatite solution and the reaction mixture was stirred for 24 hours at room temperature. pH 11 was maintained for the whole reaction time. After completion of the reaction, the mixture was filtered under vacuum and washed with deionized water (3x 50mL). The obtained silver doped HAP nanoparticles (*C-Ag-HAP*) were dried at 200°C for 12 hours. Part of the obtained sample was calcined at 1000°C (*C-Ag-HAP-sint*).

2. Synthesis of AgNO_3 doped Hydroxyapatite (Ag-HAP, Ag-HAP-sint)

The solution of 0.015M AgNO_3 (25mL) was added to the solution of 0.135 M calcium nitrate tetrahydrate (225mL). The resulted mixture was sonicated for 10 minutes, then a solution of 0.09 M of diammonium hydrogen phosphate solution (250mL) was added using a peristaltic pump (25 ml/min). The pH of the solution was adjusted to 11 and stirred continuously for 24 hours at room temperature. After the reaction time, it was filtered under vacuum, washed with deionized water, dried at 200°C for 12 hours, and part of the sample was calcined at 1000°C.

3. Preparation of silver complex-doped hydroxyapatite (Co-Ag-HAP-noncal, Co-Ag-HAP-cal600°C, Co-Ag-HAP-cal800°C)

For the preparation of the diamine-silver hydroxide complex, into the solution of AgNO_3 in ammonia (25%) was added until the precipitation of silver oxide. The mixture was centrifuged and the obtained silver oxide was redissolved in 5mL of ammonia solution (25%).

Hydroxyapatite was prepared as described in section 1. To the solution of calcium nitrate tetrahydrate and diammonium hydrogen phosphate the silver hydroxide solution was added. The pH of the reaction mixture was adjusted to 11 with ammonia solution, stirred continuously for 24 hours at room temperature, filtered, washed, dried and the resulting sample was then divided into three parts. The first sample was not calcined *Co-Ag-HAP-noncal*, while

the second and third samples were calcined at 600°C *Co-Ag-HAP-sint600°C* for 1 hour. The third sample was calcined at 800°C for another 1 hour (*Co-Ag-HAP-cal800°C*).

Solid state method

Preparation of the solid phase Ag-Hap (Sp-Ag-HAP)

The preparation of the hydroxyapatite was achieved using the steps described in section 1. For preparation of HAP nanoparticles a 0.09M $(\text{NH}_4)_2\text{HPO}_4$ (pH 11) was added to a 0.15M $\text{Ca}(\text{NO}_3)_2$ (pH 11) solution using a peristaltic pump with a flow rate of 25mL/min. The reaction mixture was stirred for 24 hours at room temperature. pH 11 was maintained for the whole reaction time. After completion of the reaction, the mixture was filtered under vacuum and washed with deionized water.

1.1 g of the obtained hydroxyapatite and 0.22g of AgNO_3 were crushed to a fine powder in an Agate mortar, and the resulting powder was calcined at 500°C (1 hour) and then 800°C (1 hour). After calcination, the previously white sample turned brown.

ACKNOWLEDGMENTS

The authors would like to express their gratitude to Dr. Lucian Barbu-Tudoran, (Babeş-Bolyai University, Cluj-Napoca) and Dr. Oana Cadar (Research Institute for Analytical Instrumentation, Cluj-Napoca) for experimental support.

REFERENCES

1. T. Ivankovic; H. Turk; J. Hrenovic; Z. Schauerperl; M. Ivankovic; A. Ressler, *J. Hazard. Mater.*, **2023**, 458, 131867.
2. A. Luceri; R. Francese; D. Lembo; M. Ferraris; C. Balagna, *Microorganisms*, **2023**, *11*(3), 629.
3. B. Le Ouay; F. Stellacci, *Nano Today*, **2015**, *10*(3), 339–354.
4. A. Gibała; P. Żeliszewska; T. Gosiewski; A. Krawczyk; D. Duraczyńska; J. Szaleniec; M. Szaleniec; M. Oćwieja, *Biomolecules*, **2021**, *11*(10), 1–20.
5. S. Durdu; E. Yalçın; A. Altinkök; K. Çavuşoğlu, *Sci. Rep.*, **2023**, *13*(1), 1–13.
6. M. L. W. Knetsch; L. H. Koole, *Polymers (Basel)*, **2011**, *3*(1), 340–366.
7. W. T. J. Ong; K. L. Nyam, *Saudi J. Biol. Sci.*, **2022**, *29*(4), 2085–2094.
8. L. Owen; K. Laird, *J. Appl. Microbiol.*, **2021**, *130*(4), 1012–1022.
9. S. P. Rivera-Sánchez; I. D. Ocampo-Ibáñez; J. A. Silva-Leal; L. J. Flórez-Elvira; A. V. Castaño-Hincapié; A. Dávila-Estupiñan; J. I. Martínez-Rivera; A. Pérez-Vidal, *Sci. Rep.*, **2020**, *10*(1), 1–7.

10. S. S. Jeremiah; K. Miyakawa; T. Morita; Y. Yamaoka; A. Ryo, *Biochem. Biophys. Res. Commun.*, **2020**, 533(1), 195–200.
11. Q. He; J. Lu; N. Liu; W. Lu; Y. Li; C. Shang; X. Li; L. Hu; G. Jiang, *Nanomaterials*, **2022**, 12(6), 1–13.
12. P. N. J. Arjun; B. Sankar; K. V. Shankar; N. V. Kulkarni; S. Sivasankaran; B. Shankar, *Coatings*, **2022**, 12, 11.
13. G. Wei; P. X. Ma, *Biomaterials*, **2004**, 25(19), 4749–4757.
14. R. Barabás; E. de Souza Ávila; L. O. Ladeira; L. M. Antônio; R. Tötös; D. Simedru; L. Bizo; O. Cadar, *Arab. J. Sci. Eng.*, **2020**, 45(1), 219–227.
15. N. Kantharia; S. Naik; S. Apte; M. Kheur; S. Kheur; B. Kale, *J. Dent. Res. Sci. Dev.*, **2014**, 1(1), 15.
16. R. Barabás; M. Rigó; M. Eniszné-Bódogh; C. Moisa; O. Cadar, *Studia UBB Chemia*, **2018**, 63(3), 137–154.
17. A. Sobczak-Kupiec; A. Drabczyk; W. Florkiewicz; M. Głąb; S. Kudłacik-Kramarczyk; D. Słota; A. Tomala; B. Tyliczszak, *Materials (Basel)*, **2021**, 14, 9.
18. J. S. Cho; D. S. Yoo; Y. C. Chung; S. H. Rhee, *J. Biomed. Mater. Res. - Part A*, **2014**, 102(2), 455–469.
19. P. Yang; Z. Quan; C. Li; X. Kang; H. Lian; J. Lin, *Biomat.*, **2008**, 29(32), 4341–4347.
20. N. A. S. Mohd Pu'ad; R. H. Abdul Haq; H. Mohd Noh; H. Z. Abdullah; M. I. Idris; T. C. Lee, *Mater. Today Proc.*, **2019**, 29, 233–239.
21. Z. Khurshid; M. S. Zafar; S. Hussain; A. Fareed; S. Yousaf; F. Sefat, *Handb. Ion. Substituted Hydroxyapatites*, 237–257, **2019**.
22. S. S. A. Abidi; Q. Murtaza, *UPB Sci. Bull. Ser. B Chem. Mater. Sci.*, **2013**, 75(3), 3–12.
23. C. S. Ciobanu; S. L. Iconaru; M. C. Chifiriuc; A. Costescu; P. Le Coustumer; D. Predoi, *Biomed Res. Int.*, **2013**.
24. P. N. Lim; E. Y. Teo; B. Ho; B. Y. Tay; E. S. Thian, *J. Biomed. Mater. Res. - Part A*, **2013**, 101 A, 9, 2456–2464.
25. J. Suwanprateeb; F. Thammarakcharoen; K. Wasoontarat; W. Chokeyivat; P. Phanphiriya, *J. Mater. Sci. Mater. Med.*, **2012**, 23(9), 2091–2100.
26. M. Roy; G. A. Fielding; H. Beyenal; A. Bandyopadhyay; S. Bose, *ACS Appl. Mater. Interfaces*, **2012**, 4(3), 1341–1349.
27. M. Vukomanović; I. Bračko; I. Poljanšek; D. Uskoković; S. D. Škapin; D. Suvorov, *Cryst. Growth Des.*, **2011**, 11(9), 3802–3812.
28. M. Li; M. J. Mondrinos; X. Chen; M. R. Gandhi; F. K. Ko; P. I. Lelkes, *J. Biomed. Mater. Res. Part A*, **2006**, 79(4), 963–73.
29. N. Iqbal; M. R. Abdul Kadir; N. A. N. Nik Malek; N. Humaimi Mahmood; M. Raman Murali; T. Kamarul, *Mater. Lett.*, **2012**, 89, 118–122.
30. N.-I. Farkas; L. Marinçaş; L. Barbu-Tudoran; R. Barabás; G. L. Turdean, *J. Funct. Biomater.*, **2023**, 14(6), 331.
31. P. Narendran; A. Rajendran; M. Garhnayak; L. Garhnayak; J. Nivedhitha; K. C. Devi; D. K. Pattanayak, *Colloids Surf. B Biointerfaces*, **2018**, 169, 143–150.
32. R. Barabás; N. I. Farkas; C. L. Nagy; O. Cadar; C. Moisa; L. Bizo, *Ceram. Int.*, **2021**, 47(6), 8584–8592.
33. V. R. Dejeu; B. Reka; A. M. Cormoş; B. E. Sára; P. Ş. Agachi, *Studia UBB Chemia*, **2010**, 55(2, 1), 179–188.